

# Electrical and Thermoelectrical Properties of $\text{TlIn}_{1-x}\text{Yb}_x\text{Te}_2$ ( $0 \leq x \leq 0.10$ ) Solid Solutions in the Temperature Range of 80–1000 K

F.F. ALIEV<sup>a,\*</sup>, E.R. YUZHASHOV<sup>a</sup>, U.M. AGAYEVA<sup>b</sup> AND M.M. ZARBALIEV<sup>b</sup>

<sup>a</sup>Institute of Physics of ANAS, Baku, av. H. Javid 131, AZ1143, Azerbaijan

<sup>b</sup>Sumgayit State University, Azerbaijan

(Received March 10, 2015; revised version June 22, 2015; in final form October 20, 2015)

The temperature dependence of the electrical conductivity  $\sigma$ , the Hall coefficient  $R$  and the thermopower coefficient  $\alpha$  in the solid solutions  $\text{TlIn}_{1-x}\text{Yb}_x\text{Te}_2$  ( $0 \leq x \leq 0.10$ ) have been investigated in the temperature range of 80–1000 K. The effective masses of electrons and holes have been determined on the basis of the kinetic parameters. It was established that starting from  $x=0.05$  the solid solutions of  $\text{TlIn}_{1-x}\text{Yb}_x\text{Te}_2$  belong to narrow-gap semiconductors having high values of the interaction matrix element. It is shown that the samples of  $\text{TlIn}_{1-x}\text{Yb}_x\text{Te}_2$  in the region of  $0.10 \geq x \geq 0.05$  are promising materials for the energy converters operating at high temperatures.

DOI: [10.12693/APhysPolA.129.69](https://doi.org/10.12693/APhysPolA.129.69)

PACS: 71.20.Nr, 72.15.Jf

## 1. Introduction

Sufficiently intensive studies of electrical and thermoelectric properties of  $\text{TlIn}_{1-x}\text{Yb}_x\text{Te}_2$  solid solutions [1–6] are connected primarily with the use of these materials in a variety of energy converters and, particularly in the manufacture of thermoelectric transducers operating at high temperatures.

According to [1] the solubility region of  $\text{TlYbTe}_2$  in  $\text{TlInTe}_2$  at room temperature is up to 10%. Transition from  $\text{TlInTe}_2$  to  $\text{TlIn}_{1-x}\text{Yb}_x\text{Te}_2$  is accompanied by the increase of hole concentration. The increase of the hole concentration is connected with arising of various structural imperfections, vacancies and anti-structure defects in those alloys; emerging intrinsic defects, mainly vacancies, are electroactive.

Another characteristic feature of the  $\text{TlIn}_{1-x}\text{Yb}_x\text{Te}_2$  solid solutions is that the substitution of the indium atoms by ytterbium ones allows to vary the width of the band gap  $E_g$  from 0.70 (at  $x=0$ ) to 0.54 eV ( $x=0.1$ ). Such substitution leads to a substantial changes of charge carriers concentration and hence the electrical and thermoelectrical properties of the material. The implementation of the technological methods allow to reduce the hole concentration up to  $10^{18} \text{ cm}^{-3}$ , i.e., it is possible to control electric and thermoelectric properties of the material by controlling the process of substitution of indium atoms by ytterbium ones. Studies of electrical, thermal and thermoelectric properties of  $\text{TlIn}_{1-x}\text{Yb}_x\text{Te}_2$  solid solutions show that these materials may successfully be used in many energy converters operating at high temperatures in the infrared (IR) range.

## 2. Synthesis of samples

The synthesis of  $\text{TlInTe}_2$ – $\text{TlYbTe}_2$  solid solutions was conducted by fusing the initial components taken in stoichiometric ratio. For the synthesis there were used high purity materials (99.999–99.992%). According to the constitution diagram [1], a minor deviation from stoichiometry in any direction may result in heterophase samples. Therefore, the batch was added up to 0.05 mass% of tellurium over the stoichiometric requirement. The synthesis was carried out in the evacuated to  $10^{-2}$  Pa, and sealed quartz ampoules in the following way: the temperature of the heater with quartz ampoules containing substance, was being raised at a rate of 20–25 K/h up to 750 K. The samples were kept for 3–4 h at this temperature and then were being heated to 1100 K and kept for another 4 h. The melt was then shaken during heating several times to accelerate the diffusion of constituents through each other. After homogenization lasting for 20–25 h at 1250 K the ampoule was moved with the speed of 2–3 mm/h through the zone with a temperature gradient of 50 K/cm.

The obtained ingots were cooled slowly (2 K/h) to 1000 K and then down to 500 K at a rate of 4 K/h, after which the furnace was turned off. For reaching more homogenization the synthesized materials were ground into powder, properly mixed and charged into ampoules. Evacuated and sealed ampoules were placed into the furnace, heated up 1250 K and kept for 2–3 h, depending on the Yb content. Then they were slowly cooled to the annealing temperatures 950–1100 K and kept for 50–90 h, depending on the Yb content.

As a result single crystals and large-block polycrystalline  $\text{p-TlIn}_{1-x}\text{Yb}_x\text{Te}_2$  were obtained. The measurements were performed on polycrystalline samples, because the given study was aimed to obtain thermoelectric materials with maximum figures of merit. The amount

\*corresponding author; e-mail: [farzali@physics.ab.az](mailto:farzali@physics.ab.az)

of ytterbium in samples was assessed by calculations of return factor for Yb atoms in  $\text{TlIn}_{1-x}\text{Yb}_x\text{Te}_2$ , which is equal to  $\approx 0.5$ .

### 3. Results and discussion

#### 3.1. Determination of the band parameters of $\text{TlIn}_{1-x}\text{Yb}_x\text{Te}_2$ on the basis of kinetic coefficients

On the basis of measurements of the temperature dependences of electrical conductivity  $\sigma$ , the Hall coefficient  $R$  and thermopower coefficient  $\alpha$  (Figs. 1–3) of  $\text{TlIn}_{1-x}\text{Yb}_x\text{Te}_2$  ( $0 \leq x \leq 0.10$ ) solid solutions in the temperature range of 80–1000 K, effective masses of electrons and holes were determined. As seen from Fig. 1, the  $\sigma(T)$  dependences for different compositions of the solid solutions are substantially unlike one another. The region of intrinsic conduction for the initial compound  $\text{TlInTe}_2$  begins at the temperature  $\approx 700$  K while the intrinsic region shifts towards higher temperatures with increase in relative content of ytterbium in  $\text{TlIn}_{1-x}\text{Yb}_x\text{Te}_2$  solid solutions. The width of thermal band gap ( $E_{g0}$ ) at  $T = 0$  K for the investigated samples was determined from slopes of the curves  $\lg\sigma = f(10^3/T)$  in high temperature region: it was revealed that with increasing Yb content in the solid solutions  $E_{g0}$  changes from 0.70 eV for the initial compound  $\text{TlInTe}_2$  up to 0.54 eV for  $\text{TlIn}_{0.90}\text{Yb}_{0.10}\text{Te}_2$ .

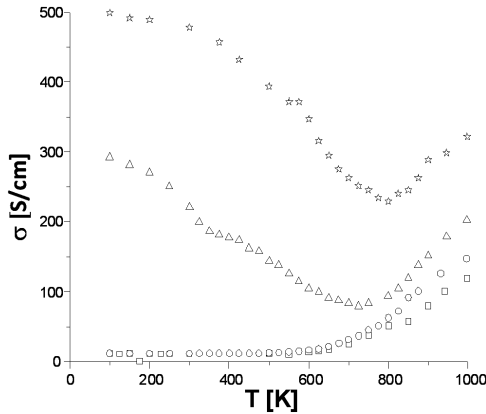


Fig. 1. Temperature dependences of electrical conductivity in  $\text{TlIn}_{1-x}\text{Yb}_x\text{Te}_2$ ;  $\square$  — ( $x = 0$ ),  $\circ$  — ( $x = 0.02$ ),  $\Delta$  — ( $x = 0.05$ ),  $*$  — ( $x = 0.10$ ).

Figures 2 and 3 show temperature dependences of the Hall coefficient  $R$  and thermopower coefficient  $\alpha$  in  $\text{TlIn}_{1-x}\text{Yb}_x\text{Te}_2$  solid solutions. The signs of both coefficients are positive and this proves that conduction occurs by holes.

It is seen from Fig. 2 that the Hall coefficient decreases with increasing Yb content in the solid solutions and accordingly, hole concentration goes up. At  $T > 700$  K the region of intrinsic conduction is detected for all samples. Starting from  $x = 0.05$  further increasing Yb content leads to a shift of the region of intrinsic conduction towards higher temperatures. This phenomenon is also observed in the temperature dependence of  $\alpha$  (Fig. 3): it

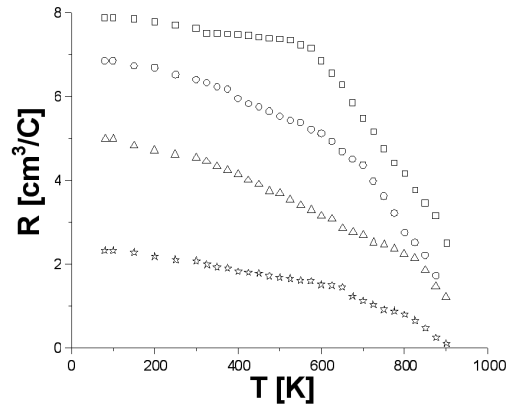


Fig. 2. Temperature dependence of Hall coefficient (at  $H = 1200$  A/m) in  $\text{TlIn}_{1-x}\text{Yb}_x\text{Te}_2$ . Markers describing experimental points correspond to the values of  $x$  as in Fig. 1.

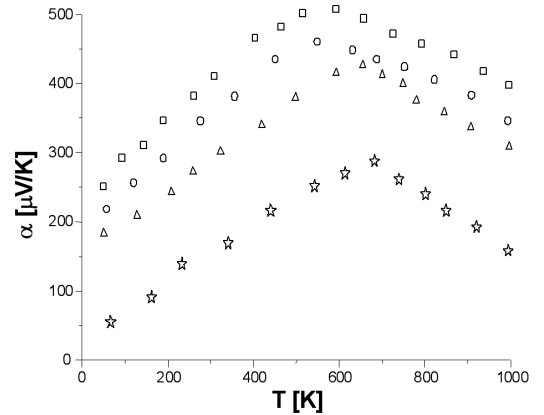


Fig. 3. Temperature dependences of thermopower coefficient in  $\text{TlIn}_{1-x}\text{Yb}_x\text{Te}_2$ . Markers describing experimental points correspond to the values of  $x$  as in Fig. 1.

is seen that  $\alpha(T)$  grows linearly up to  $T \approx 650$  K and then decreases in the intrinsic region. It can be seen from Figs. 2–3 that starting from  $x \geq 0.05$  the peculiarities of temperature dependences of  $\sigma(T)$  and  $\alpha(T)$  have the same pattern as for narrow-gap semiconductors [7], namely temperature dependences of  $\sigma$  and  $\alpha$  have inverse character. From this point of view the corresponding experimental data obtained in [5] seem inconsistent.

Weak dependence of  $R(T)$  and linear dependence of  $\alpha(T)$  up to  $T \approx 650$  K in these samples indicates that the conduction occurs mainly by one type ( $p$ -type) of charge carriers; so we can determine an effective mass of holes from the following expression, which is valid for the thermopower coefficient in a classically strong magnetic field for the case of square law of dispersion of charge carriers having any degree of degeneration [8]:

$$\alpha_{\infty} = -\frac{k}{e} \left[ \frac{5}{3} \frac{F_{3/2}(\eta^*)}{F_{1/2}(\eta^*)} - \eta^* \right], \quad (1)$$

where  $k = 0.86 \times 10^{-4}$  eV/K, the Boltzmann constant;  $\eta^*$  — reduced chemical potential,  $F(\eta^*)$  — one-parameter Fermi–Dirac integral. It is known that ther-

mopower at a strong magnetic field is expressed like this:  $\alpha_\infty = \alpha + \Delta\alpha_\infty$ , where  $\Delta\alpha_\infty$  — magneto-thermopower in a classically strong magnetic field. In the narrow-gap semiconductors  $\Delta\alpha_\infty$  is  $\approx 10$ – $12\%$  of the value  $\alpha$  [9].

The Hall coefficient in a strong magnetic field ( $R_\infty$ ) is determined only by the concentration of charge carriers

$$R_\infty = \frac{1}{ep}. \quad (2)$$

In its turn the said concentration of holes is expressed through the relationship below [8]:

$$p = 4\pi \left( \frac{2m_p^*kT}{h^2} \right)^{3/2} F_{3/2}(\eta^*), \quad (3)$$

where  $m_p^*$  — effective mass of holes.

The effective masses of holes  $m_p^*$  were determined from (3) through known values of  $p$ ,  $T$  and  $\eta^*$  and the obtained data are given in Table I. As seen from Table I effective masses of holes in the investigated temperature range for all samples weakly depend on temperature. It points to the fact that valence band of  $\text{TlIn}_{1-x}\text{Yb}_x\text{Te}_2$  obeys square law of dispersion.

Degeneration of holes ceases at  $T \geq 700$  K and begins intrinsic conduction which is displayed by the experimental curves shown in Figs. 1–3. A value of intrinsic concentration of charge carriers in the region of intrinsic conduction is determined from electroneutrality equation  $N_a = p - n$  as

$$n_i = 4.9 \times 10^{15} (m_n^* m_p^*)^{3/4} T^{3/2} \exp\left(\frac{-E_g}{2kT}\right), \quad (4)$$

where  $n_i$  is determined from dependences  $R(T)$  and  $\sigma(T)$  in the region of intrinsic conduction. In the case of two types of charge carriers  $R$  and  $\sigma$  in weak magnetic fields are determined by the following expressions [10]:

$$\left. \begin{aligned} R &= \frac{1}{N_a e} \frac{(1-c)(1-b^2c)}{(1+bc)^2} \\ \sigma &= N_a e b \mu_p \frac{1+bc}{b(1-c)} \end{aligned} \right\}, \quad (5)$$

where  $c = n_i/(N_a + n_i)$ ,  $b = \mu_n/\mu_p$  — ratio of electron mobility to hole mobility. Values of  $N_a$  can be found from the initial part of  $R(T)$  curve on which  $R$  does not depend on temperature.

The equality  $r_n = r_p$  ( $r_n, r_p$  — scattering factors) is valid for the case where the dependence of electron relaxation time and hole relaxation time on energy is the same [8]. In this case  $b$  does not depend on temperature. Temperature dependence of hole mobility is determined in the form:  $\mu_p(T) = \mu_p(100 \text{ K})T^{-0.7}$ , where  $\mu_p(100 \text{ K}) = R\sigma(100 \text{ K})$ . By solving the system (5), values of  $c$  and  $b$  were found and then a value of intrinsic concentration  $n_i$  was assessed.

On the basis of values of  $n_i$ ,  $m_p^*$  and  $E_g$  in (4) it is possible to determine an effective mass of electrons ( $m_n^*$ ) (see Table I). Electron concentration  $n$  may be determined from the formula (3) written for electrons.

Another important parameter of semiconductors is a value of temperature coefficient of the width of band gap  $\alpha_1 = dE_g/dT$ . Linearly diminishing  $E_g$  with tem-

TABLE I

Energetic band parameters and thermo-physical parameters of  $\text{TlIn}_{1-x}\text{Yb}_x\text{Te}_2$  solid solutions. Here,  $\alpha_1 = dE_g/dT \times 10^{-4}$  [eV K $^{-1}$ ] — temperature coefficient of the width of band gap;  $E_{g0}$  [eV] — the width of thermal band gap at  $T = 0$  K;  $m_n^*$  and  $m_p^*$  — effective masses of electrons and holes, correspondingly;  $\chi_{\text{ph}}$  [ $\times 10^{-2}$  W cm $^{-1}$  K $^{-1}$ ] — coefficient of phonon thermal conductivity;  $\chi_{\text{tot}}$  [ $10^{-2}$  W cm $^{-1}$  K $^{-1}$ ] — coefficient of total thermal conductivity;  $\Delta W_i$  [cm K W $^{-1}$ ] — coefficient of thermal resistance;  $\Gamma$  ( $\times 10^3$ ) — parameter of disorder.

$x$	$\alpha_1$	$E_{g0}$	$T$	$E_g(T)$	$m_n^*$	$m_p^*$	$\chi_{\text{ph}}$	$\chi_{\text{tot}}$	$\Delta W_i$	$\Gamma$
0	1.2	0.70	100	0.70	0.040	0.55	0.98	0.98		
			300	0.66	0.040	0.53	0.95	0.95		
			500	0.64	0.040	0.53	0.79	0.80		
			600	0.63	0.039	0.52	0.73	0.78		
			700	0.62	0.038	0.51	0.68	0.75		
			800	0.60	0.037	0.51	0.62	0.76		
			900	0.59	0.036	0.50	0.60	0.78		
0.02	1.23	0.66	100	0.65	0.036	0.52	0.86	0.87	14	2.9
			300	0.62	0.036	0.52	0.82	0.83	16	
			500	0.60	0.035	0.51	0.64	0.67	29	
			600	0.59	0.035	0.51	0.60	0.66	50	
			700	0.57	0.034	0.50	0.58	0.68	58	
			800	0.56	0.033	0.49	0.54	0.70	69	
			900	0.55	0.032	0.48	0.47	0.74	78	
0.05	1.28	0.62	100	0.61	0.034	0.48	0.76	0.83	29	7.1
			300	0.58	0.034	0.47	0.63	0.78	35	
			500	0.56	0.033	0.47	0.58	0.72	49	
			600	0.54	0.032	0.46	0.56	0.70	58	
			700	0.53	0.031	0.45	0.55	0.72	69	
			800	0.52	0.030	0.45	0.51	0.74	76	
			900	0.50	0.029	0.44	0.46	0.78	84	
0.10	1.3	0.54	100	0.53	0.031	0.47	0.66	0.78	49	12.3
			300	0.52	0.031	0.47	0.42	0.75	133	
			500	0.50	0.030	0.46	0.37	0.76	143	
			600	0.48	0.029	0.46	0.32	0.78	183	
			700	0.46	0.028	0.46	0.30	0.85	200	
			800	0.44	0.027	0.45	0.29	0.88	237	
			900	0.42	0.026	0.45	0.24	0.94	255	

perature is typical for narrow-gap semiconductors, since temperature coefficient of the width of forbidden gap  $\alpha_1$  is negative. In this case dependence  $E_g(T)$  may be expressed in the form

$$E_g(T) = E_{g0} - \alpha_1 T. \quad (6)$$

By substituting expression (6) in (4) we shall get

$$n_i T^{-3/2} = 4.9 \times 10^{15} (m_n^* m_p^*)^{3/4} e^{-\alpha_1/2k} e^{-E_g/2kT}. \quad (7)$$

From the above expression we can derive the analytical formula for  $\alpha_1$ :

$$\alpha_1 = 72.26k + 2k \left[ \frac{3}{4} \ln(m_p^* m_n^*) + \frac{3}{2} \ln T - \ln n_i \right] - E_{g0}/T. \quad (8)$$

The calculated values for  $\alpha_1$  have been given in Table I, too.

Therefore, in the investigated temperature range  $\text{TlIn}_{1-x}\text{Yb}_x\text{Te}_2$  solid solution ( $0 \leq x \leq 0.10$ ) has hole conduction at severely degenerated state of hole gas. The  $\text{TlIn}_{1-x}\text{Yb}_x\text{Te}_2$  valence band obeys square law of dispersion. At  $T \geq 650$  K the intrinsic conduction region is observed and the nature of temperature dependences  $\sigma$  and  $\alpha$  is explained by the presence of two types of charge carriers. Starting from  $x = 0.05$  the temperature course  $\sigma(T)$  becomes obviously qualitatively and quantitatively different during transition from  $\text{TlInTe}_2$  to  $\text{TlIn}_{1-x}\text{Yb}_x\text{Te}_2$ . This transition is supposed to be accompanied by the transition from a semiconductor to a narrow-gap semiconductor.

### 3.2. Thermoelectric figure of merit

According to Ioffe [11], increasing the value of  $\mu/\chi_{\text{ph}}$  ( $\chi_{\text{ph}}$  — phonon part of the thermal conductivity,  $\mu$  — mobility of charge carriers) leads to an increase in  $Z$ . It means that a quantitative decrease in phonon scattering is fully compensated by an increase in scattering by defects [12]. As the wavelength of electrons is more than of phonons it leads to the total increase in  $\mu/\chi_{\text{ph}}$ . The thermoelectrical peculiarities of the  $\text{TlIn}_{1-x}\text{Yb}_x\text{Te}_2$  solid solutions show that these materials can provide rather high thermoelectrical figure of merit.

It is known that efficiency of a thermoelectric transducer is determined by the following formula:

$$Z = \alpha^2 \sigma \chi_{\text{tot}}. \quad (9)$$

Here,  $\alpha^2 \sigma$  — thermoelectrical power,  $\chi_{\text{tot}}$  — total thermal conductivity. Total thermal conductivity is determined as the sum of phonon  $\chi_{\text{ph}}$  and hole  $\chi_{\text{h}}$  thermal conductivities. Taking into account that  $\chi_{\text{h}} = L_0 \sigma T$ , where  $L_0 = (\pi^2/3)(k/e)^2 = 2.44 \times 10^{-8}$  W  $\Omega$ /K, we get

$$\chi_{\text{tot}} = \chi_{\text{ph}} + L_0 \sigma T. \quad (10)$$

According to the theoretical calculations of Leibfried and Haasen [13] at temperatures  $T > \theta$  phonon conductivity is determined as

$$\chi_{\text{ph}} = \frac{12}{5} \left( \frac{k}{h} \right)^3 \frac{\bar{M} \delta \theta^3}{\gamma_0^2 T} = 5.7 \frac{\bar{M} \delta \theta^3}{\gamma_0^2 T}, \quad (11)$$

where  $\gamma_0$  — Grüneisen constant has usually the order of 2 for the most solid state materials;  $\theta$  - Debye temperature,  $\bar{M}$  - average mass of the compound atoms,  $\delta$  - cube root of the volume per atom. For the solid solutions of  $\text{TlIn}_{1-x}\text{Yb}_x\text{Te}_2$   $\bar{M}$  can be calculated from  $\bar{M} = (1-x)(\bar{M}_{\text{TlInTe}_2} + x\bar{M}_{\text{TlYbTe}_2})/2$ , where  $\bar{M}_{\text{TlInTe}_2} = 143.60$ ,  $\bar{M}_{\text{TlYbTe}_2} = 158.15$ ;  $\theta = 20$  K [14];  $\delta = \sqrt[3]{\frac{\Omega_0}{N}}$ , where  $\Omega_0 = a^2 c$  — volume of the tetragonal unit cell,  $N$  — the number of atoms per unit volume [15]. By substituting the data into Eq. (11), we get values for  $\chi_{\text{ph}}$ , which are presented in Table I. Values of  $\chi_{\text{tot}}$ , calculated on the basis of Eq. (10) are also given in Table I. Having values of  $\chi_{\text{tot}}$ , the values of  $Z$  can be calculated according to Eq. (9) (see Table I).

For taking into consideration the influence of disorders in the lattice thermal conduction we used the theory of Klemens [16], which takes into account scattering

phonons by point defects in addition to the Umklapp scattering processes

$$\chi_{\text{ph}} = \chi_v (\omega_0/\omega_d) \arctan(\omega_d/\omega_0), \quad (12)$$

where  $\omega_0/\omega_d = k/(2\pi^2 \chi_v \omega_d A)$  and  $A = (1/4V^3 N) \Gamma$ . Here,  $\chi_v$  — thermal conductivity of the stoichiometric compound in the absence of defects' influence,  $\omega_d = \theta k/\hbar$  is the maximum frequency in the Debye model (Debye frequency),  $\omega_0$  is the frequency at which the value of relaxation times due to U-processes and scattering on defects are equal,  $V$  is average sound velocity in the crystal,  $N$  is number of atoms in a unit volume, is the parameter of disorder which is equal to

$$\Gamma = x(1-x) [(\Delta\bar{M}/\bar{M})^2 + \varepsilon \Delta\delta/\delta]^2 \quad (13)$$

and takes into consideration simultaneous influence of a local change in density and elastic properties,  $\varepsilon$  — characterizes elastic properties of medium and  $\Delta\bar{M}/\bar{M}$  is a relative change in mass when basic atoms are replaced by impurity atoms, which can be expressed as

$$\Delta\bar{M}/\bar{M} = \frac{\bar{M}_{\text{TlYbTe}_2} - \bar{M}_{\text{TlInTe}_2}}{(1-x)\bar{M}_{\text{TlInTe}_2} + x\bar{M}_{\text{TlYbTe}_2}}. \quad (14)$$

Taking into account that for the  $\text{TlIn}_{1-x}\text{Yb}_x\text{Te}_2$  ( $0 \leq x \leq 0.10$ ) solid solution the Vegard law remains in force, for computing  $\Delta\delta/\delta$  we used the following expression:

$$\frac{\Delta\delta}{\delta} = \left( \frac{a_{\text{imp}} - a_{\text{mat}}}{a_{\text{mat}}} \right) \frac{\eta}{1 + \eta}, \quad (15)$$

which was derived from the elastic continuum "sphere and hole" model, where matrix and impurity are treated as continuous isotropic media [17, 18]. Here  $a_{\text{mat}}$  and  $a_{\text{imp}}$  are parameters of elementary cell of matrix and impurity consequently and  $\eta = (1 + \nu)/[2(1 - 2\nu)]$ ,  $\nu$  — the Poisson ratio. All parameters necessary for calculations ( $v, \varepsilon, \nu, \theta, N$  etc.) were taken from (14)–(15) [19, 20] and linearly extrapolated for  $\text{TlIn}_{1-x}\text{Yb}_x\text{Te}_2$  solid solutions as  $P = (1-x)P_{\text{TlInTe}_2} + xP_{\text{TlYbTe}_2}$ , where  $P$  is a necessary parameter for calculation of thermal conductivity of the solid solutions.

It should be noted that values of  $\chi_{\text{ph}}(T)$  calculated by expressions (11) and (12) insignificantly differ. Values of the  $\Gamma$  parameter for various  $x$  in the  $\text{TlIn}_{1-x}\text{Yb}_x\text{Te}_2$  are presented in Table I. From the comparison of stoichiometric compound  $\text{TlInTe}_2$  with the solid solutions of  $\text{TlIn}_{1-x}\text{Yb}_x\text{Te}_2$  it is clear that the parameter of disorder  $\Gamma$  changes by nearly 4.3 times at room temperature. It means that for other parameters being equal, thermal resistance arising in the solid solutions due to disorder must be much more than in  $\text{TlInTe}_2$ . It gives a reason that the determined values of  $\Gamma$  are true reflection of real relation of the basic factors responsible for additional scattering of phonons by point defects. It leads to the additional thermal resistance as [17]:

$$\Delta W_i = 1/\chi_{\text{ph}} - 1/\chi_v.$$

Calculated data for  $\Delta W_i$  are also presented in Table I.

Having all necessary data set in Table I allows us to analyze the thermoelectrical peculiarities of the  $\text{TlIn}_{1-x}\text{Yb}_x\text{Te}_2$  solid solutions more precisely for the getting rather high thermoelectrical figure of merit. The

dependence of  $Z$  on the content of Yb in  $\text{TlIn}_{1-x}\text{Yb}_x\text{Te}_2$  solid solutions for fixed temperatures 300, 500 and 800 K are described in Fig. 4. As seen from the figure,  $Z$  increases both with temperature and the content of Yb in the solid solutions;  $Z$  has its minimal value for  $x = 0$  at  $T = 300$  K and maximal value for  $x = 0.1$  at 800 K.

It is clear that increasing  $\alpha$ ,  $\sigma$  and decreasing  $\chi_{\text{tot}}$  lead to an increase in the values of thermoelectrical power ( $\alpha^2\sigma$ ) and thermoelectric figure of merit ( $Z$ ). Strong influence of the content of Yb atoms on  $Z$  in the investigated solid solutions is connected with high content of intrinsic defects in the materials [12].

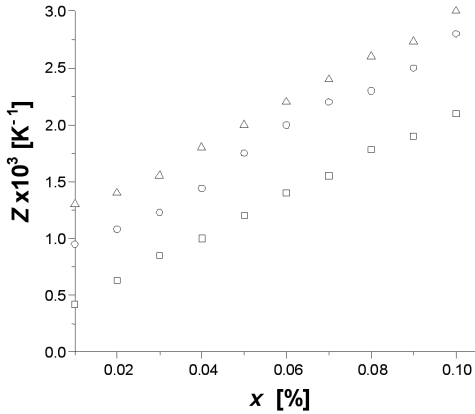


Fig. 4. The dependence of the thermoelectric figure of merit on the content of Yb in  $\text{TlIn}_{1-x}\text{Yb}_x\text{Te}_2$  solid solutions at the temperatures 300 K (□), 500 K (○) and 800 K (△).

The peculiarities of temperature dependence of  $\chi_{\text{ph}}$  also may be explained by high concentration of defects in the materials [12]. It should be noted that for the  $\text{TlIn}_{1-x}\text{Yb}_x\text{Te}_2$  solid solutions always  $\chi_{\text{ph}} > \chi_{\text{h}}$ , in spite of  $\chi_{\text{h}}$  is rising, but  $\chi_{\text{ph}}$  is decreasing with temperature in the temperature range where the material keeps its solid state.

As seen from Figs. 1 and 3,  $\sigma$  is decreasing, but  $\alpha$  is increasing in the temperature range of 300–700 K. Moreover, the concentration of holes changes insufficiently in the temperature range of 100–500 K for all investigated samples (Fig. 2). Therefore the decrease of  $\sigma$  with temperature in the above mentioned temperature range is connected to decreasing mobility of holes. The decrease of hole mobility with temperature occurs mainly due to scattering of holes on thermal lattice vibrations and defects according to  $\mu_{\text{h}} \sim T^{-0.7}$  [1, 4]. The defects arise in the  $\text{TlIn}_{1-x}\text{Yb}_x\text{Te}_2$  solid solutions mainly due to vacancies of In and Yb; at that Yb atoms' vacancies have more effect than In ones. The last is connected with the large value of screening of Yb atoms (ionic radiuses of  $R(\text{Yb}^{3+}) = 85.8$  pm,  $R(\text{In}^{3+}) = 81$  pm [21]) in the  $\text{TlIn}_{1-x}\text{Yb}_x\text{Te}_2$ . At the same time phonon–phonon and phonon–defect scattering effects bring to decrease of  $\chi_{\text{ph}}$  with temperature as  $\chi_{\text{ph}} \sim T^{-1.2}$ . With increase of Yb atoms' content in the solid solutions the values of  $\chi_{\text{ph}}$  and index  $n$  in the expression of  $\chi_{\text{ph}} \sim T^{-n}$  also decreases.

As a result for  $x \geq 0.05$  we have the following relation  $\mu_{\text{h}}/\chi_{\text{ph}} \sim T^{0.5}$ . Thus the increase of  $Z$  up to  $\approx 700$  K is due to linear increase of  $\alpha(T)$  (Fig. 3).

As seen from Table I for the temperatures  $> 700$  K rising the  $x$  brings to increase of  $\chi_{\text{tot}}$ . It is connected with high contribution of bipolar thermal conductivity ( $\chi'$ ) into the total heat conductivity. Therefore, for the temperatures  $> 700$  K its contribution to the total heat conductance is more than 40%. Thus at that case the expression (10) may be rewritten as  $\chi_{\text{tot}} = \chi_{\text{ph}} + \chi'$ , where  $\chi' = (\sigma_n + \sigma_p)L_0T$ .

#### 4. Conclusion

The  $\text{TlIn}_{1-x}\text{Yb}_x\text{Te}_2$  solid solutions are perspective material for practical using in the thermoelectrical transducers due to the following features:

The wavelength of holes is greater than wavelength of phonons and this fact brings to higher values of  $Z$ .

It was established that starting from  $x = 0.05$  the solid solutions of  $\text{TlIn}_{1-x}\text{Yb}_x\text{Te}_2$  belong to narrow-gap semiconductors having high values of the interaction matrix element.

It is shown that the samples of  $\text{TlIn}_{1-x}\text{Yb}_x\text{Te}_2$  in the region of  $0.10 \geq x \geq 0.05$  are promising materials for the energy converters operating at high temperatures.

Due to the peculiar defect structure of the  $\text{TlIn}_{1-x}\text{Yb}_x\text{Te}_2$  solid solutions the condition of  $\mu_{\text{h}}/\chi_{\text{ph}} \gg 1$  for the charge carriers and phonons is fulfilled, which result in gaining maximal values for  $Z$ .

The increase of the rate of substitution of In atoms with Yb ones leads to an increase in the values of thermoelectrical power ( $\alpha^2\sigma$ ) and thermoelectric figure of merit ( $Z$ ).

#### References

- [1] M.M. Zarbaliyev, *Neorg. Mater.* **35**, 560 (1999) (in Russian).
- [2] E.M. Orujov, E.M. Gojayev, R.A. Kerimova, *Fiz. Tverd. Tela* **48**, 40 (2006) (in Russian).
- [3] L.D. Ivanova, Yu.V. Petrova, Yu.V. Granatkina, T.E. Svehkova, M.A. Korzhayev, V.S. Semiskov, *Neorg. Mater.* **43**, 1436 (2007) (in Russian).
- [4] M.M. Zarbaliyev, *Izv. AN Azerb. Repub. Fiz.* **5**, 26 (1999) (in Russian).
- [5] E.M. Gojayev, R.A. Kerimova, *Neorg. Mater.* **40**, 1314 (2004) (in Russian).
- [6] M.M. Zarbaliyev, A.M. Akhmedova, U.M. Zarbaliyeva, *Vestnik Bak. Gos. Univ.* **1**, 1435 (2011) (in Russian).
- [7] S.I. Radautsan, E.K. Arutanov, V.I. Pruglo, *Semimetals and narrow-gap semiconductors*, Sh-tinitsa, Kishinev 1979 (in Russian).
- [8] B.M. Askerov, *Kinetic effects in semiconductors*, Nauka, Leningrad 1970 (in Russian).
- [9] F.F. Aliev, H.A. Hasanov, *Ind. J. Phys.* **87**, 345 (2013).
- [10] F.F. Aliev, E.M. Kerimova, S.A. Aliev, *Fiz. Tekh. Poluprovodn.* **36**, 932 (2002) (in Russian).

- [11] A.F. Ioffe, *Semiconductor thermoelements*, Izd. AN USSR, Moskva 1960 (in Russian).
- [12] V.S. Oskotskiy, I.I. Smirnov, *Defects in crystals and thermoconductivity*, Nauka, Leningrad 1972 (in Russian).
- [13] G.I. Leibfried, P. Haasen, *Z. Phys.* **137**, 67 (1954).
- [14] E.M. Gojayev, M.M. Zarbaliev, M.M. Kurbanov, A.B. Naqiev, D.D. Bayramov, *Neorg. Mater.* **23**, 163 (1987) (in Russian).
- [15] V.A. Hajiyev, M.M. Kurbanov, *Neorg. Mater.* **26**, 1325 (1990) (in Russian).
- [16] P.G. Klemens, *Phys. Rev.* **119**, 507 (1960).
- [17] B. Abeles, *Phys. Rev.* **131**, 1906 (1963).
- [18] J.D. Eshelby, in: *Collected Works of J.D. Eshelby: The Mechanics of Defects and Inhomogeneities*, Eds. X. Markenscoff, A. Gupta, Springer, Dordrecht 2006, p. 259.
- [19] E.M. Kerimova, *Crystal physics of low-dimensional chalcogenides*, Elm, Baku 2012 (in Russian).
- [20] M.M. Zarbaliev, *Neorg. Mater.* **40**, 1314 (2004) (in Russian).
- [21] K.N.R. Taylor, M.I. Darby, *Physics of Rare Earth Solids*, Chapman and Hall Ltd., London 1972.